Archives of Hydro-Engineering and Environmental Mechanics
Vol. 50 (2003), No. 4, pp. 381–400

A Simple Model of Sinking of Breakwater due to Earthquake-Induced Subsoil Liquefaction

Andrzej Sawicki

Institute of Hydro-Engineering of the Polish Academy of Sciences,
ul. Kościerska 7, 80-953 Gdańsk, Poland, e-mail: as@ibwpan.gda.pl

(Received July 24, 2003; revised September 22, 2003)

Abstract

The paper deals with engineering analysis of breakwater behaviour due to earthquake-induced subsoil liquefaction. First, a simple model enabling analysis of pore-pressure generation in saturated granular soils, due to cyclic loading, is outlined. It is also shown how this model can be applied to the analysis of seabed behaviour during earthquakes. Then, a simple model of breakwater resting on saturated subsoil in which the phenomena of pore-pressure generation and liquefaction take place is described. This model enables estimation of changes of seabed effective reaction due to pore-pressure generation, as well as subsequent sinking of the breakwater due to subsoil liquefaction. Numerical examples illustrate theoretical considerations and show links between breakwater behaviour and earthquake characteristics.

Key words: liquefaction, marine structures, cyclic loadings, earthquake sinking

1. Introduction

The present paper was inspired by the effects of the 1999 Turkey earthquake which strongly damaged the Kocaeli region, including coastal zone of the Izmit Bay, which is part of the Marmara Sea. The observed effects of this earthquake include: sinking of breakwaters and other structures, large displacements of quay-walls in harbours, large settlements of ground and backfills, etc., Sumer et al (2002). The global cost of devastation was enormous, as can be measured by the billions of US dollars, not to mention many thousands of human lives.

Understanding and prediction of earthquake effects is one of the main challenges in contemporary civil and maritime engineering, as it may lead to safer design of infrastructure. This is not an easy task since earthquakes are usually unexpected, therefore detailed observation of associated phenomena is practically impossible. Some observations can be made during post-earthquake inspections, which is the main source of information about permanent global effects of ground shaking.

The aim of this paper is an engineering analysis of breakwater settlements due to earthquake-induced subsoil liquefaction. In fact we analyse the behaviour of a rigid block, which may model a breakwater, gravity jetty or other structures. For the sake of brevity, a designation of breakwater will be used in the present paper. In order to describe this behaviour, some knowledge regarding the mechanism of pore-pressure generation in saturated soil is necessary, as this process leads to liquefaction. Therefore, at the beginning of this paper, a brief description of earthquake-induced liquefaction of seabed is presented. A simple model of breakwater resting on saturated subsoil, in which the phenomena of pore pressure generation and liquefaction take place, is then described. The model enables estimation of regrouping of effective stresses in subsoil, as well as assessment of subsequent sinking of the breakwater due to subsoil liquefaction. Numerical examples illustrate theoretical considerations and show links between breakwater behaviour and earthquake characteristics.

We have attempted to construct a model of the system: breakwater-subsoil as simple as possible, using methods of general mechanics, and minimal set of available information. It is shown that such an approach provides realistic predictions, which are also of practical importance.

2. Earthquake-Induced Liquefaction of Seabed

Saturated granular soil is usually treated as a two-phase medium consisting of a solid skeleton and fluid which fills pores. Overall behaviour of such a mixture depends on the effective stresses in the soil skeleton. If they are compressive and not exceeding certain criteria as, for example, the Coulomb-Mohr yield condition, the soil skeleton is able to support additional loads, and behaves macroscopically like a solid body. Under certain conditions such as, for example cyclic loadings, the pore-water pressure may increase, reducing the effective stresses, and consequently also reducing the shearing resistance of saturated soil. Under extreme conditions, the effective stresses drop to zero and saturated soil is said to have liquefied, as it behaves macroscopically as liquid, which cannot support any load.

The problem of soil liquefaction has been one of the biggest challenges in contemporary soil mechanics for some 40 years, although the first attempt to explain this phenomenon was made by Casagrande (1936) much earlier. It is impossible in this short paper to present extensive state-of-the-art regarding developments of this interesting subject. Respective references can be found in Bazant and Krizek (1976), Cakmak (1987), Finn (1982), Finn et al (1971), Ishihara and Towhata (1982), Ishihara (1996), Martin and Seed (1982), Nemat-Nasser and Shokooh (1979), Seed and Lee (1966), Valanis and Read (1982), Zienkiewicz et al (1978), Zienkiewicz et al (1999).

For purposes of this paper, it does not matter which approach, empirical or theoretical, will be used in order to determine development of liquefaction in the

seabed, provided that a method applied leads to realistic predictions. It should be mentioned that, up to now, none of existing approaches has been accepted as reliable geotechnical standard. However, for the sake of self-consistency of this paper, a simple low-resolution model enabling estimation of pore-pressure generation and liquefaction will be outlined. This model was proposed by Sawicki (1987) as alternative to computationally more complex model of Morland and Sawicki (1983, 1985). Some applications of these models to the analysis of earthquake-induced pore-pressure generation and liquefaction in saturated subsoil are described in Sawicki and Morland (1985), Sawicki and Świdziński (1989a, b).

2.1. Model of Liquefaction

The first constitutive equation describes compaction of soil in fully drained conditions

$$\frac{d\Phi}{dN} = D_1 J \exp(-D_2 \Phi), \tag{1}$$

where Φ is irreversible porosity change due to cyclic loading, defined as follows:

$$\Phi = \frac{n_0 - n}{n_0}, \tag{2}$$

where

- n – current porosity,
- n_0 – initial porosity,
- N – number of loading cycles (assumed as continuous variable),
- J – second invariant of the tensor of cyclic strain amplitudes,
- D_1 and D_2 – constants for given sand (determined from cyclic simple shear experiments).

It is assumed that there is an analogy between the compaction in fully drained conditions and the pore-pressure generation in the same soil but loaded in undrained conditions:

$$u = \frac{n_0}{\kappa(1 - n_0)}\Phi = \frac{1}{\kappa^*}\Phi, \tag{3}$$

where u = excess pore pressure (hydrostatic pressure is a reference level), κ = compressibility of the soil skeleton.

The second constitutive equation relates the deviators of the stress and strain amplitudes tensors:

$$\hat{T}^{dev} = (G_1 + G_2\sqrt{p'})\hat{E}^{dev} = 2G\hat{E}^{dev}, \tag{4}$$

where $p' = p'_0 - u$ = mean effective stress, p'_0 = initial mean effective stress, G_1 and G_2 = parameters (experimentally determined).

Eq. (4) displays degradation of 'generalized shear modulus' G during the pore-pressure generation, when the mean effective stress decreases. According to this model, as u increases the cyclic strains also increase, as observed in experiments. In the simplest interpretation, liquefaction occurs when $p' = 0$.

2.2. Earthquake-Induced Stresses and Pore-Pressure

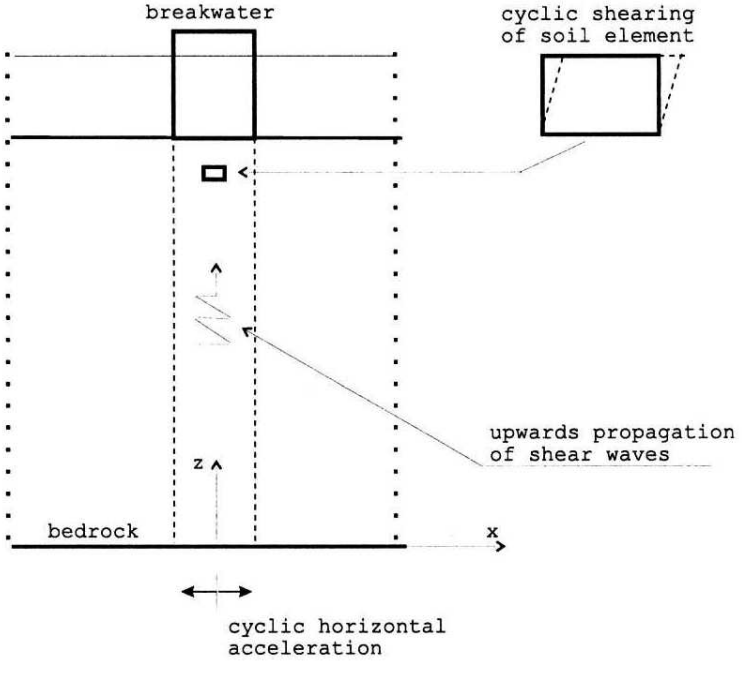

Fig. 1. Propagation of shear waves and horizontal shaking of ground during earthquake

Fig. 1 illustrates a general situation of breakwater during earthquake. The main exciting force, acting on seabed, is caused by horizontal cyclic acceleration of bedrock due to earthquake. As a result of this shaking, shear waves propagate upwards inducing the cyclic shear stresses at each point of the soil stratum. Because of the rather short duration of earthquake (42 seconds in the case of Kocaeli earthquake), there is no time for pore-pressure dissipation, and therefore undrained conditions are justified. In the first approximation, the problem may be considered as uni-axial, see 'column' of soil supporting the breakwater in Fig. 1. Distribution of the shear stress amplitudes τ_0, assuming harmonic oscillations, is given by the following differential equation:

$$\frac{d^2\tau_0}{dZ^2} + \frac{\varsigma}{G}\tau_0 = 0, \tag{5}$$

$$\varsigma = \frac{\rho\omega^2 H^2 E_0}{p_0}, \tag{6}$$

where:

$Z = z/H$	–	non-dimensional vertical co-ordinate;
H	–	depth of soil stratum;
ρ	–	density of soil-water mixture;
ω	–	frequency of earthquake-induced acceleration;
$E_0 = 10^{-3}$	–	strain unit;
$p_0 = 10^5$ N/m^2	–	stress unit;
G	–	see Eq. (4).

The boundary conditions are the following:

$$\tau_0(Z = 1) = 0, \tag{7}$$

$$\frac{d\tau_0}{dZ}(Z = 0) = \frac{\rho H A_0}{p_0} = \upsilon_0, \tag{8}$$

where A_0 = amplitude of bedrock acceleration.

Eq. (5) should be solved numerically, taking into account also Eqs. (1)–(4), using the finite differences method or another, as the mean effective stress, and therefore the soil mechanical properties are non-uniformly distributed with depth. As a result of computations, the changes of cyclic stress and strain amplitudes, as well as changes of the effective stresses are obtained as functions of N, or the real time t. Examples of computations are presented in already quoted references. It should be mentioned that it is also possible to include into numerical procedure the pore-pressure dissipation effects which relax purely undrained conditions, see Sawicki and Świdziński (1989b).

According to the model presented, the processes of pore-pressure generation and liquefaction depend on few quantities which include the soil mechanical properties (D_1, D_2, κ, G) and the intensity of ground shaking (A_0). In the case of partially undrained conditions, as well as in the analysis of pore-pressure dissipation after earthquake, the subsoil's permeability k is also a key parameter.

In this paper, specific solutions of the system of governing equations will not be discussed, as it has already been done, e.g. Sawicki and Świdziński (1989a, b). What is important is that we have some tools enabling estimation of pore-pressure generation and liquefaction in a saturated soil stratum during earthquake. A simple numerical example illustrating the model of liquefaction is presented in Section 6.

3. Model of Breakwater's Behaviour

Assume the simplest model of breakwater possible, which is a rigid block resting on cohesionless and weightless saturated subsoil. A plane problem is considered which means that all resultant forces are related to 1 meter of length (perpendicular to x, z plane). Fig. 2 shows the system: breakwater-subsoil in equilibrium before earthquake.

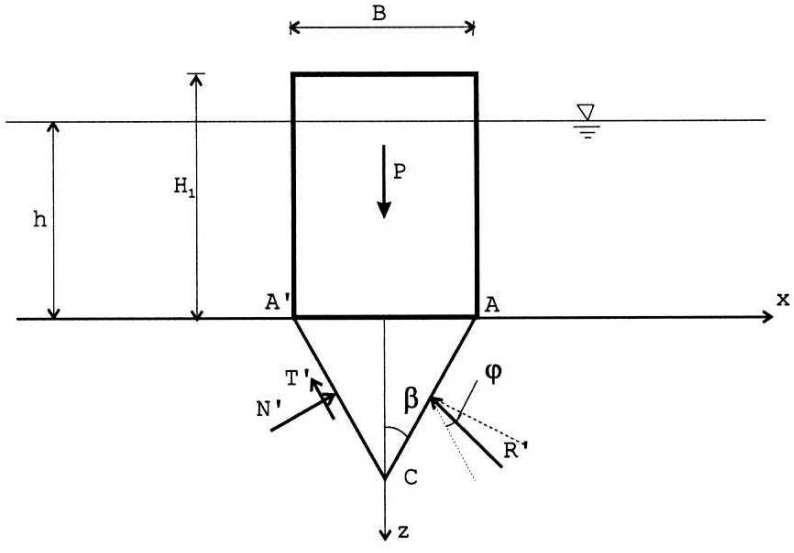

Fig. 2. Initial equilibrium of breakwater before earthquake

The distribution of initial stresses in subsoil can be determined using the methods of soil mechanics. In this Section we shall follow the methodology of soil plasticity, cf. Chen (1975). If the buoyant weight of breakwater P is large enough, the subsoil loses its bearing capacity and fails according to the well-known mechanism depicted in Fig. 3.

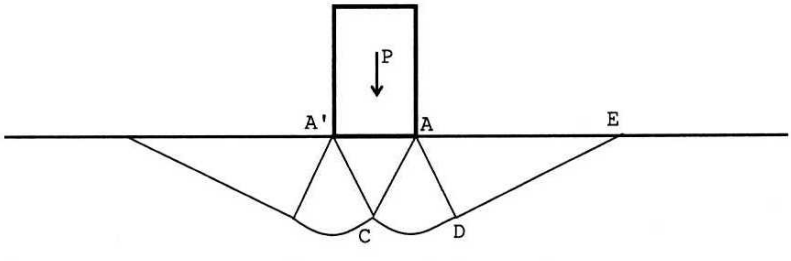

Fig. 3. Classical mechanism of subsoil failure according to plasticity solutions

It is important that just beneath a base of breakwater, a rigid wedge ACA′ which is formed moves downwards together with breakwater, pushing out the soil from adjacent regions ACD and ADE (the problem is symmetrical with respect to the z axis). In this extreme case, the resultant of soil reaction R' acting on wedge ACA′ (Fig. 2) is located on the friction cone, i.e. the following condition is satisfied:

$$T' = N' \tan \varphi = \mu N', \tag{9}$$

where: T'= component of R' tangent to surface AC (and obviously to A′C due to symmetry), N' = component of R' perpendicular to surface AC, φ = angle of internal friction.

In stages preceding the subsoil's failure, this resultant reaction should be located within the friction cone, as shown in Fig. 2, which means that failure criterion has not been reached on surfaces AC and A′C. This corresponds to working conditions of well designed structure. As P = const, the breakwater's subsoil is stable under static loading conditions. In this paper, water-waves induced stresses in seabed will be neglected for the sake of simplicity.

During the earthquake-induced pore-pressure generation, different scenarios of subsoil's behaviour are possible. In the case of 'weak earthquake', some pore-pressures are generated in subsoil, but they are rather low to cause serious damage as, for example, sinking of breakwaters and other objects. In the case of 'strong' earthquake, liquefaction of the subsoil takes place, which may lead to minor or even serious damages of coastal structures. The distinction between 'weak' and 'strong' earthquake depends on its magnitude and duration. This problem is illustrated in Section 6.

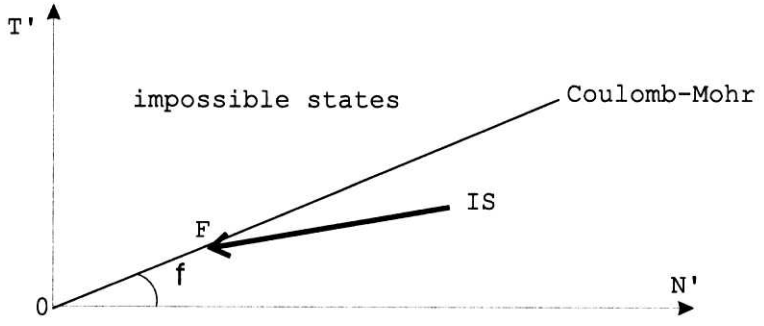

Fig. 4. Changes of subsoil reaction during pore-pressure generation

Fig. 4 illustrates changes of subsoil reaction during pore-pressure generation. Point IS (initial state) corresponds to the initial equilibrium of breakwater, before eathquake. In this case, the effective resultant of subsoil reaction R' is located within the friction cone. Recall that the initial distribution of hydrostatic

pore-pressures is treated as a reference level. At the beginning of pore-pressure generation, the value of R' and its inclination change, which corresponds to path IS–F in Fig. 4. Point F corresponds to the situation when R' reaches the friction cone (Coulomb-Mohr failure criterion is satisfied). If the pore-pressure is still generated, R' will remain on the friction cone, but its value will be decreasing (path F0 in Fig. 4). Point 0 corresponds to subsoil liquefaction since $R' = 0$.

Fig. 4 also helps in understanding of what we mean by 'weak' or 'strong' earthquake. If a given earthquake produces excess pore-pressures causing changes of R' which correspond to path IS–F, the breakwater will remain stable, as there do not exist physical conditions enabling subsoil failure. Therefore, an earthquake which generates pore-pressures not exceeding path IS–F may be regarded as 'weak' from the view point of breakwater stability. Such physical conditions for possible failure are created when R' remains on the friction cone (path F0 in Fig. 4). Possible mechanism of failure, according to plasticity solutions, is shown in Fig. 3. During this stage, probably some settlements of breakwater will take place, but there does not exist a simple method which would enable estimation of these settlements.

Sophisticated elasto-plastic models of soils are of little practical value, at the present stage of their development, for many reasons, cf. Bolton (2000), Kolymbas (2000), Sawicki (2003a). The main point of these reasons is that most of these models do not provide realistic predictions of strains, even for simple loading paths realised in laboratory conditions, see Saada and Bianchini (1989), Sawicki (2003b). The other important reasons are the following: difficult calibration of these models, their complicated structure, expensive applications (finite element analyses) which lead to uncertain results, etc. In the present paper, these possible plastic settlements of breakwater will be neglected in comparison with the settlements resulting from sinking of breakwater in liquefied subsoil.

4. Regrouping of Effective Stresses in Subsoil

First, the initial subsoil's reaction R' will be determined. It is assumed that the vertical stress imposed by buoyant weight of breakwater σ_z^0 is uniformly distributed at its base, Fig. 5. The vertical component of reaction R' can easily be determined from elementary equilibrium, i.e. $R'_z = P/2$. The horizontal component of this reaction R'_x will be determined from the assumption that the horizontal effective stress beneath the foundation is given by the following relation:

$$\sigma'_x = K_0 \sigma'_z, \tag{10}$$

where K_0 = coefficient of earth pressure at rest. Respective stresses acting on surface element AC (see Fig. 5) are the following:

$$X' = \sigma'_x \cos\beta, \; Z' = \sigma'_z \sin\beta, \tag{11}$$

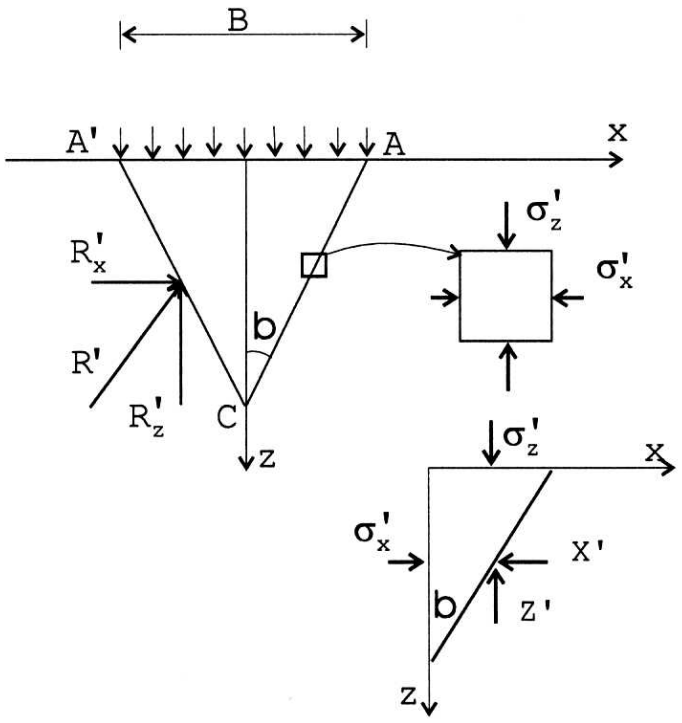

Fig. 5. Simplified stress state at surface AC

where $\beta = 45° - \varphi/2$ and $\sigma_z' = \sigma_z^0$ at initial equilibrium. Therefore, we have

$$R_x' = X'L, \quad R_z' = Z'L, \tag{12}$$

where $L = B/2\sin\beta$ = length of sector AC.

The normal and tangent components of subsoil reaction (see Fig. 2) are the following:

$$N' = R_x' \cos\beta + R_z' \sin\beta, \tag{13}$$

$$T' = -R_x' \sin\beta + R_z' \cos\beta. \tag{14}$$

At initial equilibrium, there is $T'/N' = \tan\varphi$.

During the pore-pressure generation, the effective stresses change according to the following relations:

$$\sigma_z' = \sigma_z^0 - u, \tag{15}$$

$$\sigma_x' = K_0\sigma_z^0 - u. \tag{16}$$

The soil mechanics sign convention is applied, where compression is treated as positive. The changes of effective stresses cause respective changes of subsoil's reaction, so Eqs. (12) assume the following form:

$$R'_x = (K_0\sigma_z^0 - u)L\cos\beta, \tag{17}$$

$$R'_z = (\sigma_z^0 - u)L\sin\beta. \tag{18}$$

Eqs. (17) and (18) are valid until the condition (9) is reached, which corresponds to point F in Fig. 4. Excess pore-pressure corresponding to this situation can be determined from Eqs. (9), (13), (14), (17) and (18). Explicit formula for this pore-pressure is the following:

$$u = u^* = \sigma_z^\circ\left[\left(\sin^2\beta + K_0\cos^2\beta\right) - \frac{(1-K_0)}{\mu}\sin\beta\cos\beta\right] = \varsigma\sigma_z^\circ. \tag{19}$$

Eq. (19) provides important information regarding possible, earthquake-induced failure of breakwater. Such a failure would be impossible if the maximum pore-pressure generated by earthquake $u_{\max} < u^*$.

In the case of $u = u^*$, resultant R' is located on the surface of the friction cone, which means that shearing resistance on surfaces AC and A'C has been reached. Since that, some plastic deformations of subsoil are possible, but we neglected them in the first approximation discussed in this paper. More important problem is further generation of pore-pressure which does not change the direction of R' but only influences its value (path F0 in Fig. 4). Respective changes of R' can be calculated from a simple equilibrium shown in Fig. 6. The asterisk will be used to distinguish values of respective resultants at point F (see Fig. 4).

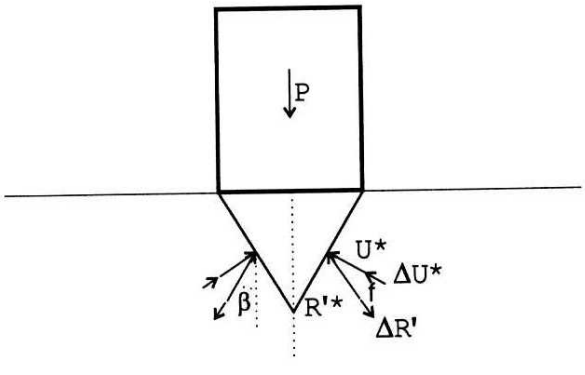

Fig. 6. Equilibrium of breakwater during pore-pressure generation, path F0 in Fig. 4

At the beginning of this stage, we have

$$R'^* \cos\beta + U^*\cos(\beta + \varphi) = P/2, \tag{20}$$

where $U^* = u^* L = u^* B/2 \sin\beta$ = resultant of excess pore-pressure. But there is also:

$$\left(R'^* + \Delta R'\right) \cos\beta + \left(U'^* + \Delta U\right) \cos\left(\beta + \varphi\right) = P/2, \tag{21}$$

where $\Delta R'$ = increment of subsoil's reaction, ΔU = increment of the resultant of pore-pressure acting on surface AC. Simple manipulations lead to the following relation:

$$\Delta R' = -\Delta u B \left(\cos\beta - \sin\beta \tan\varphi\right) = -\xi B \Delta u, \tag{22}$$

which shows how the resultant subsoil's reaction decreases when additional pore-pressure is generated. Subsoil's liquefaction begins when

$$R' = R'^* + \Delta R' = 0. \tag{23}$$

Substitution of Eq. (22) into Eq. (23) gives explicit formula for the finite increment of pore-pressure, corresponding to the onset of liquefaction:

$$\Delta u = \Delta u^{**} = \frac{1}{\xi B} R'^*. \tag{24}$$

This is the second important result, as it shows that subsoil liquefaction begins when the earthquake-induced pore-pressure reaches the value:

$$u = u^{**} = u^* + \Delta u^{**}. \tag{25}$$

After this, the pore-pressure cannot be generated, as the saturated subsoil behaves macroscopically as liquid. At this moment, the conditions enabling sinking of breakwater in a liquefied subsoil have been created.

5. Sinking of Breakwater

5.1. Governing Equations

In order to analyse breakwater settlements during subsoil liquefaction, let us consider the simplest possible one-dimensional model, shown in Fig. 7. Liquefied soil is treated as a mixture, characterized by unit weight:

$$\gamma_m = (1 - n)\, \gamma_s + n \gamma_w, \tag{26}$$

where γ_s = unit weight of solid grains, γ_w = unit weight of water.

The breakwater begins to sink in this heavy liquid when the resultant subsoil's reaction $R' = 0$, which is equivalent to vanishing of effective stresses. Vertical movement of breakwater is measured from a level of seabed. The main forces acting on breakwater are the following: Q = its own weight, S = added mass

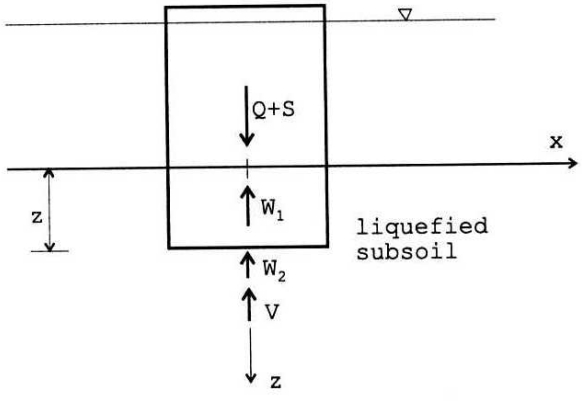

Fig. 7. Sinking of breakwater in liquefied subsoil

of adjacent water and mixture, W_1 = buoyancy in water, W_2 = buoyancy in liquefied subsoil, $V = \eta dz/dt$ = resultant of viscous damping forces, η = averaged coefficient of viscosity. For the sake of simplicity it is assumed that:

$$W_1 = \gamma_w (H_1 - z) B, \tag{27}$$

$$W_2 = \gamma_m z B, \tag{28}$$

$$S = \frac{B}{2g}[\gamma_w H_1 + (\gamma_m - \gamma_w) z]\frac{d^2z}{dt^2} \cong \frac{B}{2g}\gamma_w H_1 \frac{d^2z}{dt^2}. \tag{29}$$

Basic newtonian mechanics leads to the following differential equation describing the vertical motion of breakwater:

$$\frac{d^2z}{dt^2} + a_1\frac{dz}{dt} + a_2 z = f, \tag{30}$$

where

$$a_1 = \frac{\eta g}{Q + a_3}, \quad a_2 = \frac{g B (\gamma_m - \gamma_w)}{Q + a_3}, \quad f = \frac{g (Q - B H_1 \gamma_w)}{Q + a_3}, \quad a_3 = B H_1 \gamma_w / 2.$$

The following are the initial conditions:

$$z(t = 0) = 0, \quad v(t = 0) = \frac{dz}{dt}\ (t = 0) = 0. \tag{31}$$

The solution of the problem defined by Eqs. (30) and (31) is the following:

$$z = \frac{f}{(\lambda_1 - \lambda_2) a_2}\left(\lambda_2 e^{\lambda_1 t} - \lambda_1 e^{\lambda_2 t}\right) + \frac{f}{a_2}, \tag{32}$$

$$v = \frac{dz}{dt} = \frac{f\lambda_1\lambda_2}{(\lambda_1 - \lambda_2)a_2}\left(e^{\lambda_1 t} - e^{\lambda_2 t}\right), \tag{33}$$

where λ_1 and λ_2 are roots of the following characteristic equation:

$$\lambda^2 + a_1\lambda + a_2 = 0. \tag{34}$$

It is assumed that these roots are real, hence the following inequality holds:

$$\Delta = a_1^2 - 4a_2 > 0. \tag{35}$$

In the case of $\Delta < 0$ or $\Delta = 0$, the shape of the general solution is different, but in this paper we shall not discuss this problem, already described in mathematical textbooks, cf. Goering (1967). The above equations are valid only during the period of subsoil liquefaction which depends on earthquake magnitude and duration, subsoil properties, etc.

5.2. Viscous Damping Force and Elementary Analysis of Sinking

In the previous section, the resultant of viscous damping forces V was introduced, which is very important part of Eq. (30). This force is the resultant of very complex interactions between the sinking body and surrounding medium. In a general case, such a problem of hydrodynamics has not been solved yet, so therefore some engineering estimations of such a behaviour will be presented.

The first assumption deals with mechanical properties of liquefied soil, which is a mixture of solid grains suspended in water. Such a mixture may be considered as a macroscopically viscous 'heavy' fluid, the properties of which depend on the concentration of solid particles, see Sumer and Fredsoe (2002). According to them, the kinematic viscosity of liquefied soil is $\nu = 400\ \mathrm{m^2/s}$, which is equivalent to the dynamic viscosity $\mu = \nu g = 0.7 \times 10^6\ \mathrm{Ns/m^2}$. There is a lack of information, whether it is a precise number, common for all types of granular soils, or it is only some rough estimate of viscosity. Anyway, it is important that the order of magnitude of this essential coefficient is known.

The second assumption deals with the mechanism of sinking, which is also an important factor enabling estimation of the viscous damping force. Little is known about such a mechanism, so for the sake of consistency of the method of analysis introduced in this paper, assume that the wedge A′CA (see Figs. 2, 5 and 6) sinks together with a block. The viscous damping force is the resultant of shearing stresses acting on the edges A′C and AC, and on submerged sides of a breakwater. Elementary calculations lead to the following expression:

$$V = \mu\left[B\frac{\cos^2\beta}{\sin\beta} + 2z\right]\frac{dz}{dt} \cong \mu B\frac{\cos^2\beta}{\sin\beta}\frac{dz}{dt} = \eta\frac{dz}{dt}. \tag{36}$$

The second, non-linear term on the RHS of Eq. (36) was neglected as it is nearly of the order of magnitude smaller than the first term, at least for typical data (cf. Section 6).

Note that a structure of Eq. (36) is similar to that describing the viscous damping force of a spherical particle in fluid:

$$f_v = 6\pi r \mu \frac{dz}{dt}, \tag{37}$$

where r = radius of a particle, see Eqs. (15.6)–(15.8) in Puzyrewski and Sawicki (1987), after some re-arrangements.

It is also interesting to consider a more elementary analysis of the problem of sinking than that presented in Section 5.1, assuming that the inertia forces can be neglected in Eq. (30) in comparison with the other members of this equation. At first look, such an assumption may seem intuitive, but numerical analysis shows that, for the data considered, it gives practically the same results as Eq. (32). This simplified solution is of the following form:

$$z = \frac{f}{a_2}\left[1 - \exp\left(-\frac{a_2}{a_1}t\right)\right]. \tag{38}$$

6. Examples

6.1. Initial State

It is assumed, for illustration, that breakwater is constructed as a reinforced concrete box filled with sand. Respective dimensions are the following: $H_1 = 11$ m, $B = 9$ m, $h = 9$ m, see Fig. 2. The average unit weight of a block is $\gamma = 0.18 \times 10^5$ N/m^3. Therefore, the submerged unit weight $P = (9 \times 11 \times 0.18 - 9 \times 9 \times 0.1) \times 1 \times 10^5 = 9.72 \times 10^5$ N, and the vertical stress at the base is $\sigma_z^0 = 1.08 \times 10^5$ N/m^2. Assume also: $\varphi = 33°$ and $K_0 = 0.45$, which correspond to medium dense sand.

Components of initial subsoil reaction R'^0 are the following (see Eqs. 12–14): $R_x'^0 = 4.028$, $R_z'^0 = 4.856$ or $N_0' = 5.86$, $T_0' = 2.35$, all in unit 10^5 N. Here, superscript/subscript '0' distinguishes the initial state just before earthquake, and superposed prime ()′ denotes effecive reaction. There $T_0'/N_0' = 0.4 < 0.649 = \tan\varphi$, which means that the breakwater's subsoil is stable.

6.2. Beginning of Subsoil Failure

The beginning of subsoil failure is initiated at point F in Fig. 4, where the respective condition for plastic failure is achieved. This point corresponds to average excess pore-pressure, generated by earthquake, $u^* = 0.2376 \times 10^5$ N/m^2 (Eq. 19). Respective components of subsoil's reaction can be determined from Eqs. (17) and (18): $R_x' = 2.059 \times 10^5$ N, $R_z' = 3.791 \times 10^5$ N. If a given earthquake generates maximum pore-pressure less than u^*, the breakwater remains stable. Assume

that this earthquake is strong enough, and additional pore-pressure is generated (path F0 in Fig. 4).

6.3. Onset of Liquefaction

Path F0 in Fig. 4 corresponds to decreasing values of R' which remains on the surface of the friction cone. As already mentioned, some plastic settlements are possible along this path, but we neglect them in the first approximation. The subsoil's liquefaction begins when $R' = 0$ which corresponds to point 0 in Fig. 4. The finite pore-pressure increment corresponding to the onset of liquefaction is given by Eq. (24). For our data we have: $\Delta u^{**} = 0.8424 \times 10^5$ N/m^2 and $u^{**} = 1.08 \times 10^5$ N/m$^2 = \sigma_z^0$ (Eq. 25). This means that the breakwater is supported by 'heavy fluid', and the conditions for its sinking have been created.

6.4. Sinking of Breakwater

Eqs. (32) and (33) describe respectively vertical displacement and velocity of the breakwater during sinking in liquefied subsoil. Unit weight of this mixture is the following: $\gamma_m = [(1 - 0.35) \times 0.265 + 0.35 \times 0.1] \times 10^5 = 0.207 \times 10^5$ N/m^3, where porosity was assumed $n = 0.35$ and unit weight of soil grains $\gamma_s = 0.265 \times 10^5$ N/m^3. The averaged coefficient of viscosity of liquefied mixture is $\eta = 10.2 \times 10^6$ Ns/m^2. Determination of this coefficient in laboratory conditions would be an interesting research task.

Coefficients appearing in Eq. (30) are the following: $a_1 = 43.96$, $a_2 = 0.4149$, $f = 3.4122$. After 4 seconds, the settlement of breakwater is 0.32 m, and after 16 seconds it approaches 1.22 m, which is a realistic result. For example, it is known that the breakwater in Eregli Fishery Port had settled some 1.5 m during the Kocaeli earthquake, see Yuksel and Ozguven (2002).

After the assumed duration of subsoil's liquefaction, its resolidification takes place and Eqs. (32) and (33) are not valid. The processes taking place during this phase are not well understood or described, so we shall not attempt to analyse this problem in the present paper.

6.5. Estimation of Earthquake-Induced Subsoil Liquefaction

Up to this point, we have not linked directly the breakwater's behaviour with any concrete earthquake. In Subsection 6.2, the average earthquake-induced pore-pressure $u^* = 0.2376 \times 10^5$ N/m^2, corresponding to initiation of subsoil's failure, was calculated. Example presented in Subsection 6.3 shows that the onset of subsoil's liquefaction, for assumed data, corresponds to $u = u^{**} = 1.08 \times 10^5$ N/m^2. Then, in Subsection 6.4, we calculated breakwater settlement during subsoil liquefaction, assuming arbitrarily its duration as 4 seconds.

Consider now the processes of pore-pressure generation and liquefaction due to some hypothetical earthquakes. The method of analysis of subsoil behaviour during earthquake is outlined in Section 2. This method will be simplified for the sake of illustration. Consider a representative soil element just beneath breakwater, assuming that distribution of stresses does not vary with depth cf. Figs. 1 and 8. Therefore, we do not have to solve the system of equations (5)–(8), but we shall consider averaged subsoil behaviour.

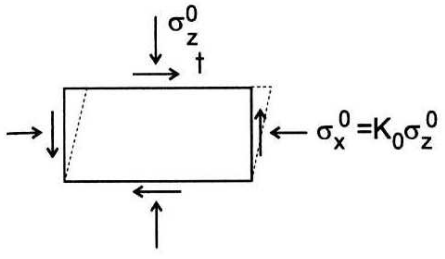

Fig. 8. Representative soil element beneath breakwater, cf. Fig. 1. Cyclic shearing during earthquake

Such element will be subjected to cyclic shearing due to earthquake. The cyclic shear stress amplitude τ_0 can be related to the amplitude of horizontal ground acceleration A_0 and to the vertical stress σ_z^0, see Ishihara (1996):

$$\tau_0 = \frac{A_0}{g}\sigma_z^0 = \alpha\sigma_z^0. \tag{39}$$

Assume also a simple, harmonic in time, earthquake history, characterized by maximum number of uniform cycles $N_{\max} = 20$ with given amplitude A_0 and period $T = 1$ second. This means that duration of earthquake is 20 seconds. In the case considered, Eqs. (1)–(4) reduce to the following differential equation describing the pore pressure generation:

$$\frac{du}{dN} = \frac{A_1\tau_0^2}{\left[G_1 + G_2\sqrt{\sigma_z^0 - u}\right]^2}\exp(-A_2 u), \tag{40}$$

where: $A_1 = D_1/4\kappa^*$, $A_2 = D_2\kappa^*$, $\tau_0 =$ Eq.(39).

In numerical calculations, the stress unit 10^5 N/m^2 will be applied. For example, $u = 1$ means that the real value of pore-pressure is 1×10^5 N/m^2. Such a convention is very useful, cf. Morland and Sawicki (1983). The following data (in respective units according to assumed convention), corresponding to medium dense sand, are assumed to be: $\kappa = 2$, $D_1 = 1.74$, $D_2 = 0.115$, $G_1 = 0.05$, $G_2 = 0.65$, see Sawicki (1991). The other data have already been presented. Eq. (40), with the initial condition $u(N = 0) = 0$, has been numerically integrated for

$\alpha = 0.2$ (medium earthquake) and $\alpha = 0.4$ (strong shaking corresponding to the Kocaeli earthquake).

Medium Earthquake

Fig. 9 shows pore-pressure generation during medium earthquake. The maximum pore-pressure generated after 20 loading cycles is $u(N = 20) = 0.219 < u^* = 0.238$ (recall respective unit!). This means that the ground motion is not strong enough to cause even some plastic settlements of breakwater, so it will remain stable during a medium earthquake.

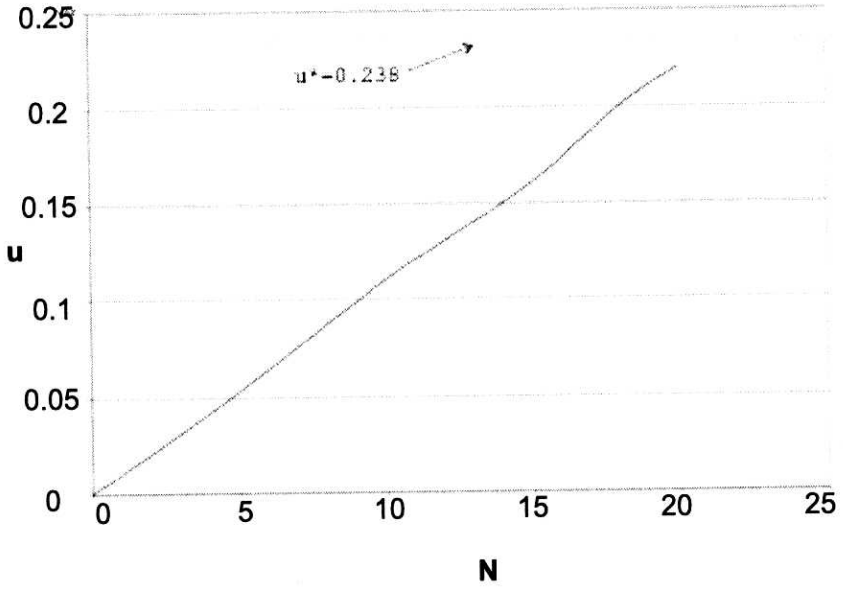

Fig. 9. Pore-pressure generation during medium earthquake

Strong Earthquake

Fig. 10 shows shows pore-pressure generated during a strong earthquake, which roughly corresponds to the Kocaeli conditions. The pore-pressure is more quickly generated than in the previous case. Just after the 6th cycle, some plastic deformations may occur. Subsoil liquefaction takes place after 16 cycles (16 seconds) and it is the beginning of sinking of the breakwater. Just 4 seconds of subsoil liquefaction is sufficient for nearly 32 cm settlement, calculated in Subsection 6.4. Note that earthquake-induced pore-pressure cannot exceed the value of u^{**}. After the earthquake, the subsoil resolidification takes place.

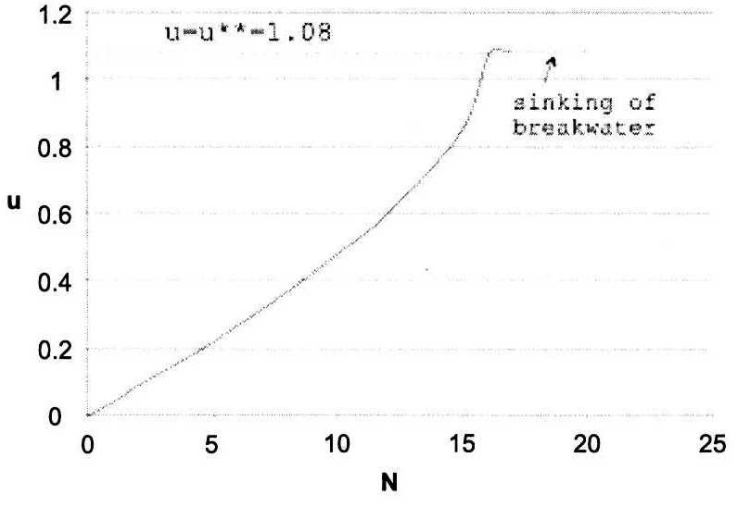

Fig. 10. Pore-pressure generation during strong earthquake

7. Conclusions

This paper is mainly of practical importance, as it shows how to simply estimate the breakwater behaviour when earthquake-induced phenomena take place in subsoil. The model of breakwater is based on simple mechanics, which should be attractive for engineers. The model needs determination of minimal possible set of parameters, which is also attractive from the practical point of view. It was shown that predictions of the model are quite realistic. The model proposed also enables understanding of processes which take place in coastal zone during earthquakes. It can also be applied to other phenomena which may take place during earthquake as, for example, sinking of buildings, piers, etc. Enclosed examples show how to deal practically with the model, and which parameters have to be determined. Some new research directions have also been pointed out. Most important of them is the detailed analysis of viscous properties of liquefied soil, as well as the study on damping forces during sinking.

Acknowledgement

This paper was written and funded within the framework of the European Union project LIMAS (Liquefaction Around Marine Structures); Contract No. EVK3-CT-2000-00038, which is kindly acknowledged. I would like to thank Professor M. Sumer, Project Co-ordinator, as well as the Steering Commitee and all

the partners involved for enabling IBW PAN participation in LIMAS. We joined the project in the fall of 2002.

References

Bazant Z. P., Krizek R. J. (1976), Endochronic Constitutive Law for Liquefaction of Sand, *Jnl Eng. Mech. Division,* ASCE, EM2, 225–238.

Bolton M. (2000), The Role of Micro-Mechanics in Soil Mechanics, *Technical Report,* CUED/D-Soils/ TR313, University of Cambridge, Department of Engineering.

Cakmak A. S., Editor (1987), *Soil Dynamics and Liquefaction,* Elsevier/Computational Mechanics Publications, Amsterdam-Oxford-New York-Tokyo.

Casagrande A. (1936), Characteristics of Cohesionless Soils Affecting the Stability of Slopes and Earthfills, *Journal of the Boston Society of Civil Engineers,* 23, 257–276.

Chen W. F. (1975), *Limit Analysis and Soil Plasticity,* Elsevier, Amsterdam.

Finn W. D. L. (1982), Dynamic Response Analyses of Saturated Sands, [in:] *Soil Mechanics – Transient and Cyclic Loads* (Editors: G. N. Pande and O. C. Zienkiewicz), John Wiley and Sons.

Finn W. D. L., Pickering D. J., Bransby P. L. (1971), Sand Liquefaction in Triaxial and Simple Shear Tests, *Jnl Soil Mech. Foundation Division,* ASCE, 97, SM4, 639–659.

Goering H. (1967), *Elementare Methoden zur Losung von Differentialgleichungsproblemen,* Akademie-Verlag, Berlin (Polish translation).

Ishihara K. (1996), *Soil Behaviour in Earthquake Geotechnics,* Clarendon Press, Oxford.

Ishihara K., Towhata I. (1982), Dynamic Response Analysis of Level Ground Based on the Effective Stress Method, [in:] *Soil Mechanics – Transient and Cyclic Loads* (Editors: G. N. Pande and O. C. Zienkiewicz), John Wiley and Sons.

Kolymbas D. (2000), The Misery of Constitutive Modelling, [in:] *Constitutive Modelling of Granular Materials* (Editor: D. Kolymbas), Springer, Berlin.

Martin P. P., Seed H. B. (1982), One-dimensional Dynamic Ground Response Analyses, *Jnl Geotechnical Engineering Division,* ASCE, 108, GT7, 935.

Morland L. W., Sawicki A. (1983), A Mixture Model for the Compaction of Saturated Sand, *Mechanics of Materials,* 2, 217–231.

Morland L. W., Sawicki A. (1985), A Model for Compaction and Shear Hysteresis in Saturated Granular Materials, *Jnl Mechanics Physics of Solids,* 33, 1–24.

Nemat-Nasser S., Shokooh A. (1979), A Unified Approach to Densification and Liquefaction of Cohesionless Sand in Cyclic Shearing, *Canadian Geotechnical Jnl,* 16, 659–678.

Puzyrewski R., Sawicki J. (1987), *Foundations of Fluid Mechanics and Hydraulics* (in Polish), PWN, Warsaw, 332 pages.

Saada A., Bianchini G., Editors (1989), *Constitutive Equations for Granular Non-Cohesive Soils,* Balkema, Rotterdam/Brookfield.

Sawicki A. (1987), An Engineering Model for Compaction of Sand under Cyclic Loading, *Rozprawy Inżynierskie (Engineering Transactions),* 35, 4, 677–693.

Sawicki A. (1991), *Soil Mechanics for Cyclic Loadings* (in Polish), IBW Publications, Gdańsk, 189 pages.

Sawicki A. (2003a), Applied Mechanics against the Arts of Geotechnical and Coastal Engineering, *Engineering Transactions,* in press.

Sawicki A. (2003b), Cam-Clay Approach to Modelling Pre-Failure Behaviour of Sand against Experimental Data, *Arch. Hydro-Eng. Env. Mech.,* 50, 3.

Sawicki A., Morland L. W. (1985), Pore Pressure Generation in a Saturated Sand Layer Subjected to a Cyclic Horizontal Acceleration at its Base, *Jnl Mech. Physics Solids,* 33, 545–559.

Sawicki A., Świdziński W. (1989a), Mechanics of a Sandy Subsoil Subjected to Cyclic Loadings, *Int. Jnl Num. Anal. Methods in Geomechanics,* 13, 511–529.

Sawicki A. and Świdziński W. (1989b), Pore Pressure Generation, Dissipation and Resolidification in a Saturated Soil, *Soils and Foundations*, 29, 1–18.

Seed H. B., Lee K. L. (1966), Liquefaction of Saturated Sands During Cyclic Loadings, *Jnl Soil Mech. Foundation Division*, ASCE, 92, SM6, 105–134.

Sumer B. M., Kaya A., Hansen N. E. (2002), Impact of Liquefaction on Coastal Structures in the 1999 Kocaeli, Turkey earthquake, *Proc. 12th Int. Offshore and Polar Eng. Conf.*, Kitakyushu, 504–511.

Sumer B. M., Fredsoe J. (2002), *The Mechanics of Scour in the Marine Environment*, World Scientific, New Jersey/Singapore/London/Hong Kong, 536 pages.

Valanis K. C., Read H. E. (1982), A New Endochronic Plasticity Model for Soils, [in:] *Soil Mechanics – Transient and Cyclic Loads* (Editors: G. N. Pande and O. C. Zienkiewicz), John Wiley and Sons, 375–417.

Yuksel Y., Ozguven O. (2002), Effects of the 1999 Kocaeli Earthquake on the Marine Structures and a Case Study; Eregli Fishery Harbour, *Workshop on Wave- and Seismic-Induced Liquefaction and Its Implications for Marine Structures*, EU Fifth Framework Programme, LIMAS, Istanbul, Book of Abstracts, 29–30.

Zienkiewicz O. C., Chang C. T., Hinton T. (1978), Nonlinear Seismic Response and Liquefaction, *Int. Jnl Num. Analyt. Methods in Geomechanics*, 2, 381–404.

Zienkiewicz O. C., Chan A. H. C., Pastor M., Schrefler B. A. and Shiomi T. (2000), *Computational Geomechanics with Special Reference to Earthquake Engineering,* John Wiley and Sons, Chichester-New York-Weinheim-Brisbane-Singapore-Toronto.